Journal of the Physical Society of Japan
Vol. 77, No. 2, February, 2008, 024713

Transient Oscillation of Currents in Quantum Hall Effect of Bloch Electrons

Manabu MACHIDA*, Jun GORYO[1]†, and Naomichi HATANO‡

Institute of Industrial Science, The University of Tokyo, Komaba, Meguro, Tokyo 153-8505
[1]*Department of Physics and Mathematics, Aoyama Gakuin University, 5-10-1 Fuchinobe, Sagamihara, Kanagawa 229-8558*

(Received August 30, 2007; accepted December 3, 2007; published February 12, 2008)

We consider the quantum Hall effect of two-dimensional electrons with a periodic potential and study the time dependence of the Hall and longitudinal currents when the electric field is applied abruptly. We find that the currents oscillate in time with very large frequencies because of quantum fluctuation and the oscillations eventually vanish, for their amplitudes decay as $1/t$.

KEYWORDS: integer quantum Hall effect, Chern number, linear response theory
DOI: 10.1143/JPSJ.77.024713

1. Introduction

It is renowned that the Hall conductance in two dimensional electron systems under a strong magnetic field is quantized to an integer or a fraction multiplied by e^2/h with very high accuracy.[1] The relations between the conductance and topological numbers were discussed extensively,[2–8] since the topological numbers take quantized values exactly. In the present paper, we discuss the integral quantization in noninteracting Bloch states. Thouless, Kohmoto, Nightingale, and den Nijs (TKNN) showed using the Kubo formula that the quantized Hall conductivity is represented by the Chern number, which is a topological number defined on the two-dimensional torus (i.e., the magnetic Brillouin zone).[2,9] The same result is also obtained from the adiabatic approximation.[10–12] It would be an intriguing issue, at least from a purely theoretical point of view, that how the topologically quantized conductivity is modified when we go beyond the Kubo formula or the adiabatic approach.

Interest in the TKNN theory was renewed recently in the field of ultra-cold atomic gases. The TKNN Hamiltonian is mapped to the Hamiltonian of a cold atomic gas trapped by a rotating optical lattice. Rotating Bose–Einstein condensates in a co-rotating optical lattice was indeed experimentally realized recently,[13] which fueled the interest in the TKNN theory. The atomic gas system does not contain any perturbative effects coming from impurities or long-range Coulomb-type interactions. Hence, compared with the electron system in the solid states, the atomic gas system is clean and the theoretical results of the TKNN theory can be applied without taking into account the corrections from such perturbations. An alternative method of applying an effective magnetic field to a cold atomic gas is also proposed.[14,15] This method utilizes the internal degrees of freedom of cold atoms instead of the rotation of the system. The Hofstadter butterfly,[16] which has been observed in a two-dimensional superlattice structure in a semiconductor heterojunction,[17–19] is predicted to be studied more easily using cold atomic gases.

In this paper, we focus on the effect of a suddenly applied dc electric field on the integer quantum Hall effect of Bloch electrons.[20] The results are readily applied to the cold atomic gas trapped by a rotating optical lattice. We calculate the resulting current with the Kubo formula.[21–24] The linear response theory for an abruptly applied dc field was particularly investigated by Greenwood.[24] We here follow Greenwood's formulation of the linear response theory.

An interesting feature of our finding is an observation of fluctuation around the quantized conductivity, which is normally considered a very rigid quantity; we find that the Hall current has a time-dependent correction to the Chern-number term in the TKNN theory. The Hall current j_x and the longitudinal current j_y oscillate in time with large frequencies because of quantum fluctuation, or oscillation between different subbands. The oscillation eventually ceases and the time-dependent Hall current converges to the Chern-number term of the TKNN theory. The amplitude of the oscillation decays as $1/t$. In the previous paper,[20] we already reported the existence of time-dependent correction terms. In the present paper, we present additional calculations particularly on the long-time behavior and on the time-dependent fields under an applied current.

This paper is organized as follows. In §2, we derive the currents in the x and y directions following Greenwood's formulation of the linear response theory. We derive the same results as in our previous paper, but under a different gauge. We also mention the correspondence between electron gases in a magnetic field and rotating cold atomic gases. In §3, we show that the time-dependent oscillation of the currents decays as $1/t$ and eventually ceases, and the Hall current approaches to a certain value obtained from the TKNN theory. Finally we give conclusions. In Appendix, we calculate electric fields under an applied current instead of currents under an applied field. We show that the voltages have similar time dependence.

2. Time Dependence of Currents

We consider noninteracting electrons in a periodic potential in the x–y plane. A magnetic field B is applied in the z direction. At time $t = 0$, we suddenly apply an electric field $\boldsymbol{E}(t)$ in the y direction. We calculate the currents of this system with the Kubo formula. The Kubo formula for a step-function external field is also known as the Greenwood linear response theory.[24]

Using the Landau gauge, we write the Hamiltonian of the system as

$$\mathcal{H} = \mathcal{H}_0 - eyE_y\theta(t), \tag{1}$$

*E-mail: machida@iis.u-tokyo.ac.jp
†E-mail: jungoryo@phys.aoyama.ac.jp
‡E-mail: hatano@iis.u-tokyo.ac.jp

where

$$\mathcal{H}_0 = \frac{1}{2m_\mathrm{e}}[p_x^2 + (p_y + eBx)^2] + V_\mathrm{p}, \tag{2}$$

$$V_\mathrm{p} = U_0 \cos\left(\frac{2\pi x}{a}\right) + U_0 \sin\left(\frac{2\pi y}{b}\right). \tag{3}$$

In our previous paper,[20] we treated the external field as a time-dependent vector potential. We here use the time-dependent scalar potential as in eq. (1). We show below that the resulting formulae are the same.

The Hamiltonian (1) can also describe a rotating dilute cold atomic gas trapped in an optical lattice.[25] To see this correspondence, let us consider a cold atom with mass m_a confined in a harmonic potential. The periodic optical lattice which traps the cold atom rotates in the z direction with angular momentum Ω. At $t = 0$, the optical lattice is tilted along the y-axis or accelerated in the y direction. The Hamiltonian of this system is written in the rotating frame as

$$\begin{aligned}\tilde{\mathcal{H}} &= \frac{1}{2m_\mathrm{a}}(p_x^2 + p_y^2) - \boldsymbol{\Omega}\cdot\boldsymbol{L} + \frac{1}{2}m_\mathrm{a}\Omega^2(x^2+y^2)\\ &\quad + V_\mathrm{p} - yV_y\theta(t),\end{aligned} \tag{4}$$

where $\boldsymbol{\Omega} = {}^\mathrm{t}(0,0,\Omega)$ and $\boldsymbol{L} = \boldsymbol{p}\times\boldsymbol{x}$. We note that the centrifugal force is canceled because the frequency of the harmonic trap is the same as the frequency of the rotation, and the interactions between atoms are neglected. Equation (4) is also expressed as

$$\begin{aligned}\tilde{\mathcal{H}} &= \frac{1}{2m_\mathrm{a}}[(p_x - m\Omega y)^2 + (p_y + m\Omega x)^2]\\ &\quad + V_\mathrm{p} - yV_y\theta(t),\end{aligned} \tag{5}$$

By substituting m_e, $eB/2m_\mathrm{e}$, and eE_y for m_a, Ω, and V_y, respectively (see Table I), we have

$$\tilde{\mathcal{H}} = \mathrm{e}^{\mathrm{i}(eB/2\hbar)yx}\mathcal{H}\mathrm{e}^{-\mathrm{i}(eB/2\hbar)yx}. \tag{6}$$

Thus, moving from the Landau gauge to the symmetric gauge by the operator $\exp[\mathrm{i}(eB/2\hbar)yx]$, we see that the Hamiltonian (1) for an electron gas is identical to the Hamiltonian (4) for a cold atomic gas.

We consider the ratio ϕ $(= \Phi/\Phi_0)$ of the flux Φ $(= Bab)$ per unit cell to the flux quanta Φ_0 $(= h/e)$. We put

$$\phi = \frac{p}{q}, \tag{7}$$

where p and q are coprime integers. Because of the presence of the periodic potential, each Landau level splits into p sublevels.

Let us first consider $\mathcal{H}_0$. We write the eigenvalues and eigenfunctions of $\mathcal{H}_0$ as

$$\mathcal{H}_0\,|\phi_{Nm}\rangle = E_{Nm}\,|\phi_{Nm}\rangle, \tag{8}$$

where the subscript N labels Landau levels and the subscript m labels sublevels in a Landau level ($1 \le m \le p$). We define

Table I. Correspondence between Hamiltonians (1) and (4).

Electron gas in a magnetic field	Rotating cold atomic gas
m_e	m_a
$eB/2m_\mathrm{e}$	Ω
eE_y	V_y

the generalized crystal momentum $\hbar\boldsymbol{k}$ in the magnetic Brillouin zone:[2] $0 \le k_x < 2\pi/qa$ and $0 \le k_y < 2\pi/b$. Note that $\mathrm{e}^{\mathrm{i}k_x qa}$ and $\mathrm{e}^{\mathrm{i}k_y b}$ are the eigenvalues of the translational operator. We define

$$\begin{aligned}\mathcal{H}_{0\boldsymbol{k}} &\equiv \mathrm{e}^{-\mathrm{i}\boldsymbol{k}\cdot\boldsymbol{x}}\mathcal{H}_0\mathrm{e}^{\mathrm{i}\boldsymbol{k}\cdot\boldsymbol{x}},\\ |\phi_{Nm}\rangle &\equiv \mathrm{e}^{\mathrm{i}\boldsymbol{k}\cdot\boldsymbol{x}}|u_{Nm}(\boldsymbol{k})\rangle,\end{aligned} \tag{9}$$

which satisfy

$$\mathcal{H}_{0\boldsymbol{k}}\,|u_{Nm}(\boldsymbol{k})\rangle = E_{Nm}(\boldsymbol{k})\,|u_{Nm}(\boldsymbol{k})\rangle. \tag{10}$$

We thus block-diagonalized the Hamiltonian $\mathcal{H}_0$ into each subspace of $\boldsymbol{k}$.

Let us consider small U_0 and treat the periodic potential as a perturbation in the subspace of a crystal momentum. Taking the lowest-order terms into account, we obtain the wave function as[2]

$$\begin{aligned}u_{Nm}(\boldsymbol{k}; x, y) &= \sum_{n=0}^{p-1} d_m^n \sum_{s=-\infty}^{\infty} \chi_N\left(x - qas - \frac{qan}{p} + k_y\ell^2\right)\\ &\quad\times \mathrm{e}^{-\mathrm{i}k_x(x-qas-qan/p)}\mathrm{e}^{-2\pi\mathrm{i}(sp+n)y/b},\end{aligned} \tag{11}$$

where $\ell = \sqrt{\hbar/eB}$ is the cyclotron radius and $\chi_N(x)$ satisfies

$$\partial_x^2\chi_N(x) = \left(\frac{x^2}{\ell^4} - \frac{2N+1}{\ell^2}\right)\chi_N(x). \tag{12}$$

We note that $u_{Nm}(\boldsymbol{k}; x, y)$ in eq. (11) satisfies the magnetic Bloch theorem:

$$\begin{aligned}u_{Nm}(\boldsymbol{k}; x+qa, y)\mathrm{e}^{2\pi\mathrm{i}py/b} &= u_{Nm}(\boldsymbol{k}; x, y)\\ &= u_{Nm}(\boldsymbol{k}; x, y+b).\end{aligned} \tag{13}$$

We have the eigenenergy within the perturbation as

$$E_{Nm}(\boldsymbol{k}) = \hbar\omega_\mathrm{c}\left(N + \frac{1}{2}\right) + \epsilon_m(\boldsymbol{k}), \tag{14}$$

where ω_c is the cyclotron frequency. Here, $\epsilon_m(\boldsymbol{k})$ and d_m^n satisfy the following secular equation (the Harper equation):[2,10]

$$\begin{aligned}&U_0\mathrm{e}^{-\pi qb/(2pa)}\cos\left(\frac{2\pi q}{p}n - \frac{qbk_y}{p}\right)d_m^n\\ &\quad + \frac{U_0}{2}\mathrm{e}^{-\pi qa/(2pb)}[d_m^{n+1}\mathrm{e}^{\mathrm{i}k_x qa/p} + d_m^{n-1}\mathrm{e}^{-\mathrm{i}k_x qa/p}]\\ &\quad = \epsilon_m(\boldsymbol{k})d_m^n.\end{aligned} \tag{15}$$

The coefficients satisfy $d_m^{n+p} = d_m^n$ and each Landau level splits into p subbands.

We consider the currents caused by the electric field $E_y\theta(t)$. In cold atomic gases, we can apply an effective electric field corresponding to $E_y\theta(t)$ either by making use of the gravitational force tilting the harmonic potential[26] or by accelerating the optical lattice.[27] We calculate the currents in the α $(= x, y)$ direction in the form

$$j_\alpha(t) = \mathrm{Tr}\,\rho(t)\frac{ev_\alpha}{qab}, \tag{16}$$

where

$$v_x = \frac{1}{m_\mathrm{e}}p_x, \quad v_y = \frac{1}{m_\mathrm{e}}(p_y + eBx). \tag{17}$$

Here $\rho(t)$ is the density operator.

Following Greenwood,[24] we expand $\rho(t)$ with respect to the electric field E_y and take the zeroth- and first-order terms into account:

$$\rho(t) \simeq \rho_0 + \rho_1(t). \tag{18}$$

The zeroth-order term ρ_0 is the initial density operator, $\mathrm{e}^{-\beta\mathcal{H}_0}/\operatorname{Tr}\mathrm{e}^{-\beta\mathcal{H}_0}$. With the help of the von Neumann equation for the density operator, ρ_1 is calculated as

$$\rho_1(t) = \frac{1}{\mathrm{i}\hbar}\int_{-\infty}^{t} \mathrm{d}t'\, \mathrm{e}^{\mathrm{i}\mathcal{H}_0(t'-t)/\hbar}\big[-eyE_y\theta(t'), \rho_0\big]\mathrm{e}^{-\mathrm{i}\mathcal{H}_0(t'-t)/\hbar}$$

$$= \frac{eE_y}{\mathrm{i}\hbar}\int_{0}^{t} \mathrm{d}t'\, \mathrm{e}^{\mathrm{i}\mathcal{H}_0(t'-t)/\hbar}\big[-y, \rho_0\big]\mathrm{e}^{-\mathrm{i}\mathcal{H}_0(t'-t)/\hbar}. \tag{19}$$

We note that the lower bound of the integral on the second line of eq. (19) is zero because of the step function in the perturbation, whereas the lower bound is negative infinity in the TKNN theory.[2] By taking the trace in eq. (16) with respect to the states in eq. (11), we obtain the currents as

$$\begin{aligned}
j_\alpha(t) &= \operatorname{Tr}\rho_1(t)\frac{ev_\alpha}{qab}\\
&= \mathrm{i}\hbar\frac{E_y e^2}{qab}\sum_{Nm}\sum_{N'm'}\int_0^{2\pi/qa}\frac{\mathrm{d}k_x}{2\pi/qa}\int_0^{2\pi/b}\frac{\mathrm{d}k_y}{2\pi/b}\frac{f_\mathrm{F}(E_{Nm}(\boldsymbol{k}))}{[E_{Nm}(\boldsymbol{k})-E_{N'm'}(\boldsymbol{k})]^2}\\
&\quad\times\Big\{\langle u_{Nm}(\boldsymbol{k})|v_{y\boldsymbol{k}}|u_{N'm'}(\boldsymbol{k})\rangle\langle u_{N'm'}(\boldsymbol{k})|v_{\alpha\boldsymbol{k}}|u_{Nm}(\boldsymbol{k})\rangle\big[1-\mathrm{e}^{-\mathrm{i}(E_{Nm}(\boldsymbol{k})-E_{N'm'}(\boldsymbol{k}))t/\hbar}\big]-\text{c.c.}\Big\}\\
&= -E_y\frac{e^2}{2\pi\hbar}\sum_{Nm}\sum_{N'm'}\int_\mathrm{MBZ}\frac{\mathrm{d}\boldsymbol{k}}{2\pi}\big[f_\mathrm{F}(E_{Nm}(\boldsymbol{k}))-f_\mathrm{F}(E_{N'm'}(\boldsymbol{k}))\big]\\
&\quad\times\operatorname{Im}\left\langle\frac{\partial u_{Nm}(\boldsymbol{k})}{\partial k_y}\,\middle|\, u_{N'm'}(\boldsymbol{k})\right\rangle\left\langle u_{N'm'}(\boldsymbol{k})\,\middle|\,\frac{\partial u_{Nm}(\boldsymbol{k})}{\partial k_\alpha}\right\rangle\big[1-\mathrm{e}^{-\mathrm{i}(E_{Nm}(\boldsymbol{k})-E_{N'm'}(\boldsymbol{k}))t/\hbar}\big],
\end{aligned} \tag{20}$$

where f_F denotes the Fermi distribution and MBZ stands for the magnetic Brillouin zone. Here we used $\mathcal{H}_{\boldsymbol{k}} = \mathrm{e}^{-\mathrm{i}\boldsymbol{k}\cdot\boldsymbol{x}}\mathcal{H}\mathrm{e}^{\mathrm{i}\boldsymbol{k}\cdot\boldsymbol{x}}$ and

$$v_{\alpha\boldsymbol{k}} = \mathrm{e}^{-\mathrm{i}\boldsymbol{k}\cdot\boldsymbol{x}}v_\alpha\mathrm{e}^{\mathrm{i}\boldsymbol{k}\cdot\boldsymbol{x}} = \frac{1}{\hbar}\frac{\partial\mathcal{H}_{\boldsymbol{k}}}{\partial k_\alpha}. \tag{21}$$

Furthermore, noting the relation $v_y = [y, \mathcal{H}_0]$, we used

$$\langle u_{Nm}(\boldsymbol{k})|\mathrm{e}^{-\mathrm{i}\boldsymbol{k}\cdot\boldsymbol{x}}y\mathrm{e}^{\mathrm{i}\boldsymbol{k}\cdot\boldsymbol{x}}|u_{N'm'}(\boldsymbol{k})\rangle = \frac{\mathrm{i}\hbar}{E_{N'm'}(\boldsymbol{k})-E_{Nm}(\boldsymbol{k})}\langle u_{Nm}(\boldsymbol{k})|v_{y\boldsymbol{k}}|u_{N'm'}(\boldsymbol{k})\rangle. \tag{22}$$

Let us put the Fermi energy in a finite gap between the m_0th and (m_0+1)st subbands which belong to the lowest Landau level ($N=0$). We consider the zero temperature. Hence the Fermi distribution satisfies $f_\mathrm{F}(E_{Nm})=1$ if $N=0$ and $m\le m_0$, and $f_\mathrm{F}(E_{Nm})=0$ otherwise. Thus we obtain

$$\begin{aligned}
j_\alpha(t) &= -2E_y\frac{e^2}{2\pi\hbar}\int_\mathrm{MBZ}\frac{\mathrm{d}\boldsymbol{k}}{2\pi}\operatorname{Im}\Bigg\{\sum_{m\le m_0}\sum_{m'>m_0}\left\langle\frac{\partial u_{0m}(\boldsymbol{k})}{\partial k_y}\,\middle|\,u_{0m'}(\boldsymbol{k})\right\rangle\left\langle u_{0m'}(\boldsymbol{k})\,\middle|\,\frac{\partial u_{0m}(\boldsymbol{k})}{\partial k_\alpha}\right\rangle\big[1-\mathrm{e}^{-\mathrm{i}(E_{0m}(\boldsymbol{k})-E_{0m'}(\boldsymbol{k}))t/\hbar}\big]\\
&\quad+\sum_{m\le m_0}\sum_{N'\ge1,m'}\left\langle\frac{\partial u_{0m}(\boldsymbol{k})}{\partial k_y}\,\middle|\,u_{N'm'}(\boldsymbol{k})\right\rangle\left\langle u_{N'm'}(\boldsymbol{k})\,\middle|\,\frac{\partial u_{0m}(\boldsymbol{k})}{\partial k_\alpha}\right\rangle\big[1-\mathrm{e}^{-\mathrm{i}(E_{0m}(\boldsymbol{k})-E_{N'm'}(\boldsymbol{k}))t/\hbar}\big]\Bigg\}\\
&= -2E_y\frac{e^2}{2\pi\hbar}\int_\mathrm{MBZ}\frac{\mathrm{d}\boldsymbol{k}}{2\pi}\operatorname{Im}\Bigg\{\sum_{m\le m_0}\sum_{m'>m_0}\left\langle\frac{\partial u_{0m}(\boldsymbol{k})}{\partial k_y}\,\middle|\,u_{0m'}(\boldsymbol{k})\right\rangle\left\langle u_{0m'}(\boldsymbol{k})\,\middle|\,\frac{\partial u_{0m}(\boldsymbol{k})}{\partial k_\alpha}\right\rangle\big[1-\mathrm{e}^{-\mathrm{i}(E_{0m}(\boldsymbol{k})-E_{0m'}(\boldsymbol{k}))t/\hbar}\big]\\
&\quad+\frac{\ell^2}{2}\sum_{m\le m_0}(\mathrm{i}\delta_{\alpha x}+\delta_{\alpha y})\big[1-\mathrm{e}^{-\mathrm{i}(E_{0m}(\boldsymbol{k})-E_{1m}(\boldsymbol{k}))t/\hbar}\big]\Bigg\},
\end{aligned} \tag{23}$$

where we used the fact that for $N'\ge1$, we have

$$\left\langle\frac{\partial u_{0m}(\boldsymbol{k})}{\partial k_y}\,\middle|\,u_{N'm'}(\boldsymbol{k})\right\rangle\left\langle u_{N'm'}(\boldsymbol{k})\,\middle|\,\frac{\partial u_{0m}(\boldsymbol{k})}{\partial k_\alpha}\right\rangle = \frac{\ell^2}{2}(\mathrm{i}\delta_{\alpha x}+\delta_{\alpha y})\delta_{N'1}\delta_{mm'}. \tag{24}$$

We can see that the time dependence of the current is due to the quantum fluctuations, or quantum oscillations between various sets of discrete levels. We ignore the quantum fluctuation between $E_{0m}(\boldsymbol{k})$ and $E_{1m}(\boldsymbol{k})$ because its frequency, which is proportional to $E_{0m}(\boldsymbol{k})-E_{1m}(\boldsymbol{k})$, is very large compared to the frequency of the fluctuation between different subbands of the lowest Landau level, which is proportional to $E_{0m}(\boldsymbol{k})-E_{0m'}(\boldsymbol{k})$. Thus we obtain

$$j_x(t) = \frac{E_y e^2}{2\pi\hbar}[N_\mathrm{Ch}+\Delta\sigma_x(t)], \tag{25}$$

$$j_y(t) = \frac{E_y e^2}{2\pi\hbar}\Delta\sigma_y(t), \tag{26}$$

where

$$N_\mathrm{Ch} = \sum_{m\le m_0}\int_\mathrm{MBZ}\frac{\mathrm{d}^2\boldsymbol{k}}{2\pi\mathrm{i}}\left(\left\langle\frac{\partial u_{0m}(\boldsymbol{k})}{\partial k_x}\,\middle|\,\frac{\partial u_{0m}(\boldsymbol{k})}{\partial k_y}\right\rangle-\text{c.c.}\right), \tag{27}$$

$$\Delta\sigma_x(t) = \sum_{m\le m_0}\sum_{m'>m_0}\int_{\mathrm{MBZ}}\frac{\mathrm{d}^2\boldsymbol{k}}{\pi}\,\mathrm{Im}\left\langle\frac{\partial u_{0m}(\boldsymbol{k})}{\partial k_y}\,\middle|\, u_{0m'}(\boldsymbol{k})\right\rangle\left\langle u_{0m'}(\boldsymbol{k})\,\middle|\,\frac{\partial u_{0m}(\boldsymbol{k})}{\partial k_x}\right\rangle \mathrm{e}^{\mathrm{i}(\epsilon_{m'}(\boldsymbol{k})-\epsilon_m(\boldsymbol{k}))t/\hbar}, \tag{28}$$

$$\Delta\sigma_y(t) = \sum_{m\le m_0}\sum_{m'>m_0}\int_{\mathrm{MBZ}}\frac{\mathrm{d}^2\boldsymbol{k}}{\pi}\left|\left\langle\frac{\partial u_{0m}(\boldsymbol{k})}{\partial k_y}\,\middle|\, u_{0m'}(\boldsymbol{k})\right\rangle\right|^2 \sin\!\left[(\epsilon_{m'}(\boldsymbol{k})-\epsilon_m(\boldsymbol{k}))t/\hbar\right]. \tag{29}$$

Note that N_{Ch} is the Chern number and takes integer values.[2,9] The time-dependent correction terms $\Delta\sigma_x(t)$ and $\Delta\sigma_y(t)$ express quantum fluctuation between different subbands of the lowest Landau level. These are expressed as the sum of different oscillating modes whose frequencies are determined by the energy difference $\epsilon_{m'}(\boldsymbol{k}) - \epsilon_m(\boldsymbol{k})$.

Hereafter, we show results of numerical calculation of the currents $j_x(t)$ and $j_y(t)$. Numerical calculation is carried out in a way similar to the Kubo formula for a dc field:[28,29] the integrals in eqs. (27), (28), and (29) are performed with random sampling of k_x and k_y. In the calculation, we set $a = b$. We here consider, for example, the following three cases: (i) $p/q = 5/4$ and $m_0 = 2$ ($N_{\mathrm{Ch}} = 2$), (ii) $p/q = 7/6$ and $m_0 = 3$ ($N_{\mathrm{Ch}} = 3$), and (iii) $p/q = 7/6$ and $m_0 = 1$ ($N_{\mathrm{Ch}} = 1$).

The band structure in the case (i) is shown in Fig. 1. In the figure, the Fermi energy that we choose is plotted with the dashed line. Figure 2 shows the currents $j_x(t)h/e^2E_y$ and $j_y(t)h/e^2E_y$ in the case (i). In the calculation, we put $U_0 = 0.1$ meV and $a = b = 100$ nm as tipical values for quantum Hall systems on a semiconductor heterojunction. The currents oscillate irregularly reflecting the fact that the energy spectra $\epsilon_{m=2}(\boldsymbol{k})$ and $\epsilon_{m=3}(\boldsymbol{k})$ in Fig. 1 strongly depend on $\boldsymbol{k}$, and $\Delta\sigma_x(t)$ and $\Delta\sigma_y(t)$ are written as the sum of sinusoidal functions with different frequencies [eqs. (28) and (29)]. The insets show the long-time behavior of the currents. As we show in the next section, $\Delta\sigma_x(t)$ and $\Delta\sigma_y(t)$ vanish for large t.

Similarly, the band structure in the cases (ii) and (iii) is shown in Fig. 3. Since N_{Ch} in eq. (27) depends on m_0, N_{Ch} changes when we change the Fermi energy. In the figure, the Fermi energy for the case (ii) is plotted with the dashed line and that for the case (iii) is plotted with the dotted line. Figure 4 shows the currents $j_x(t)h/e^2E_y$ and $j_y(t)h/e^2E_y$ in the case (ii). The currents oscillate irregularly because of contributions from different frequencies. The insets show the long-time behavior of the currents. Figure 5 shows the currents $j_x(t)h/e^2E_y$ and $j_y(t)h/e^2E_y$ in the case (iii). In this case, the currents oscillate rather regularly because the first and second subbands in Fig. 3 are almost flat, and $\Delta\sigma_x(t)$ and $\Delta\sigma_y(t)$ are almost monochromatic. The insets show the long-time behavior of the currents.

We remark the following three points. Firstly, the currents $j_x(t)$ and $j_y(t)$ are gauge invariant. We can also obtain the same results by using the time-dependent vector potential as we did in the previous paper.[20] Secondly, if a dc current instead of a voltage is abruptly turned on, the voltages in the x and y directions temporarily vary in the same manner as eqs. (25) and (26), i.e., the period of the oscillation is given by the energy difference between two sublevels (see Appendix). Finally, although the electric field is given by the step function here, we are able to calculate the time dependence of the currents for an arbitrarily time-dependent electric field by following the machinery of the Kubo formula [see eq. (A·2) below].

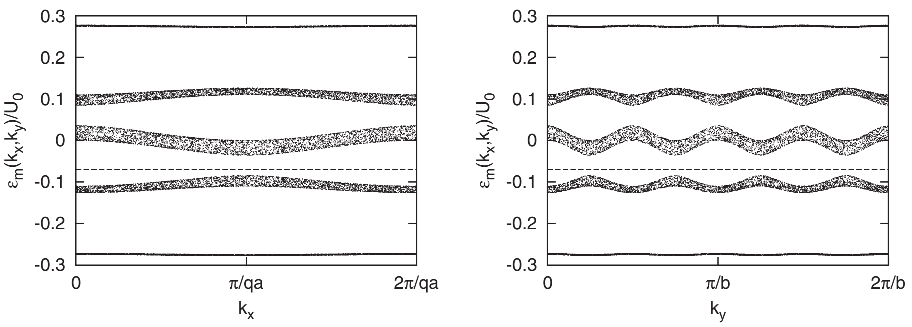

Fig. 1. Case (i): The band structure of ϵ_m as functions of k_x (left) and k_y (right). The flux ratio $p/q = 5/4$. We place the Fermi energy (the dashed line) between the second and third subbands.

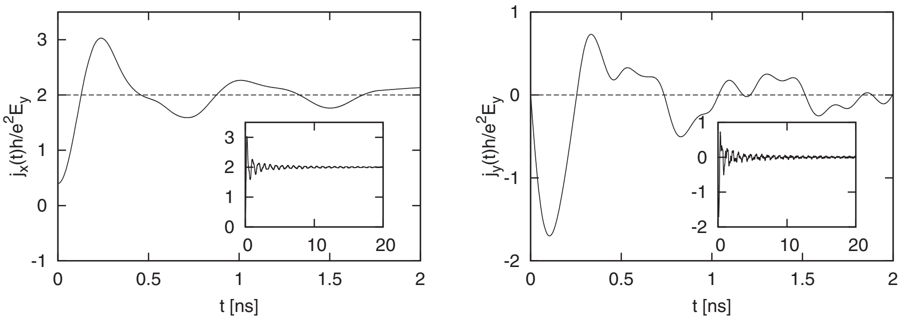

Fig. 2. Case (i): The currents $j_x(t)h/e^2E_y$ and $j_y(t)h/e^2E_y$ are shown as functions of time. We set $p/q = 5/4$, $m_0 = 2$, $U_0 = 0.1$ meV, and $a = b = 100$ nm. The dashed lines show the convergent values of $j_x(t)h/e^2E_y$ and $j_y(t)h/e^2E_y$ [N_{Ch} ($= 2$) and 0, respectively]. The insets show long-time behaviors of $j_x(t)h/e^2E_y$ and $j_y(t)h/e^2E_y$.

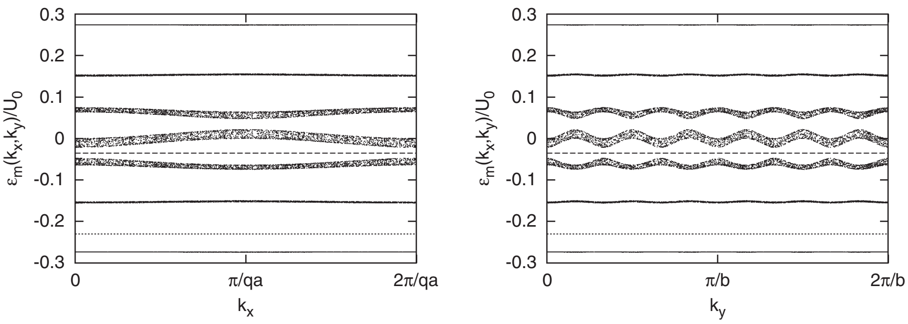

Fig. 3. Cases (ii) and (iii): The band structure of ϵ_m as functions of k_x (left) and k_y (right). The flux ratio $p/q = 7/6$. We place the Fermi energy for the case (ii) between the third and forth subbands (the dashed line), and the Fermi energy for the case (iii) between the first and second subbands (the dotted line).

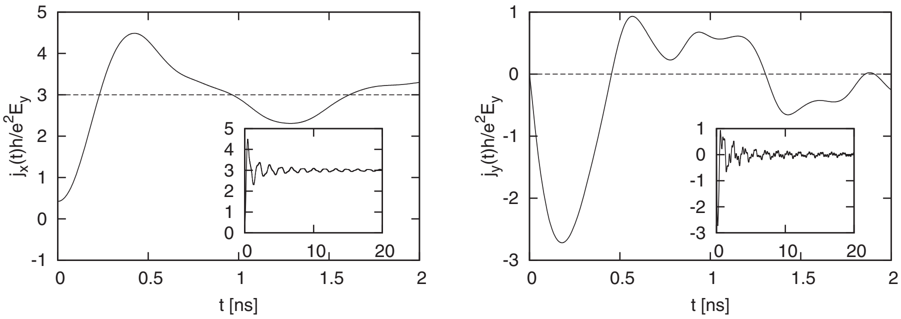

Fig. 4. Case (ii): The currents $j_x(t)h/e^2E_y$ and $j_y(t)h/e^2E_y$ are shown as functions of time. We set $p/q = 7/6$, $m_0 = 3$, $U_0 = 0.1$ meV, and $a = b = 100$ nm. The dashed lines show the convergent values of $j_x(t)h/e^2E_y$ and $j_y(t)h/e^2E_y$ [$N_{\rm Ch}$ $(= 3)$ and 0, respectively]. The insets show long-time behaviors of $j_x(t)h/e^2E_y$ and $j_y(t)h/e^2E_y$.

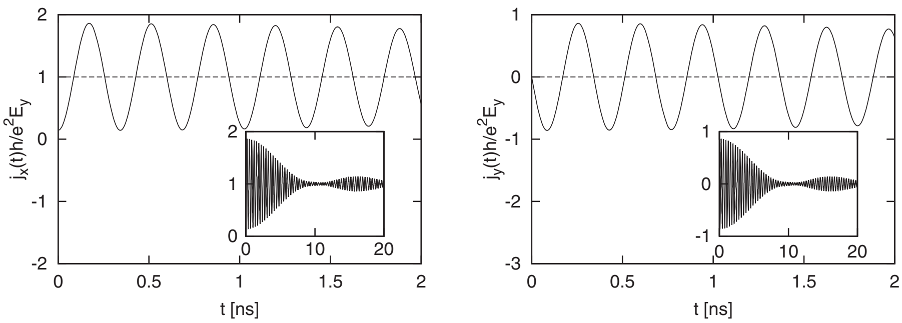

Fig. 5. Case (iii): The currents $j_x(t)h/e^2E_y$ and $j_y(t)h/e^2E_y$ are shown as functions of time. We set $p/q = 7/6$, $m_0 = 1$, $U_0 = 0.1$ meV, and $a = b = 100$ nm. The dashed lines show the convergent values of $j_x(t)h/e^2E_y$ and $j_y(t)h/e^2E_y$ [$N_{\rm Ch}$ $(= 1)$ and 0, respectively]. The insets show long-time behaviors of $j_x(t)h/e^2E_y$ and $j_y(t)h/e^2E_y$.

3. Long-Time Behavior of Currents

Let us study the currents after a long time. We show that $|\Delta\sigma_x(t)|$ and $|\Delta\sigma_y(t)|$ decay as $1/t$ using the Riemann–Lebesgue theorem:[30] $\lim_{t\to\infty}\int_{\omega_a}^{\omega_b} g(\omega)\mathrm{e}^{\mathrm{i}\omega t}\,\mathrm{d}\omega = 0$, where $g(\omega)$ is uniformly convergent.

Both $\Delta\sigma_x(t)$ and $\Delta\sigma_y(t)$ are expressed as $(\alpha = x, y)$

$$\Delta\sigma_\alpha(t) = \sum_{m\le m_0}\sum_{m'>m_0}\int_{\rm MBZ}\mathrm{d}^2\boldsymbol{k}\,\mathrm{Im}\,\bar{g}_{mm'}^{(\alpha)}(\boldsymbol{k})\mathrm{e}^{\mathrm{i}(\epsilon_{m'}(\boldsymbol{k})-\epsilon_m(\boldsymbol{k}))t/\hbar}. \quad (30)$$

We define

$$\omega_{mm'}(\boldsymbol{k}) \equiv \frac{\epsilon_{m'}(\boldsymbol{k}) - \epsilon_m(\boldsymbol{k})}{\hbar}, \quad (31)$$

$$\omega_0 \equiv \omega_{mm'}(k_x = 0, k_y), \qquad \omega_{\pi/qa} \equiv \omega_{mm'}(k_x = \pi/qa, k_y). \quad (32)$$

Hence,

$$\begin{aligned}\Delta\sigma_\alpha(t) &= 2\sum_{m\le m_0}\sum_{m'>m_0}\int_0^{2\pi/b}\mathrm{d}k_y\int_{\omega_0}^{\omega_{\pi/qa}}\mathrm{d}\omega_{mm'}\left|\frac{\partial\omega_{mm'}}{\partial k_x}\right|^{-1}\mathrm{Im}\,\bar{g}_{mm'}^{(\alpha)}(k_x,k_y)\mathrm{e}^{\mathrm{i}\omega_{mm'}t}\\ &= \sum_{m\le m_0}\sum_{m'>m_0}\mathrm{Im}\int_0^{2\pi/b}\mathrm{d}k_y\int_{\omega_a}^{\omega_b}\mathrm{d}\omega_{mm'}\,g_{mm'}^{(\alpha)}(\omega_{mm'},k_y)\mathrm{e}^{\mathrm{i}\omega_{mm'}t},\end{aligned} \quad (33)$$

where $\omega_a = \min(\omega_0, \omega_{\pi/qa})$ and $\omega_b = \max(\omega_0, \omega_{\pi/qa})$.

We note that $\int_{\omega_a}^{\omega_b} d\omega e^{i\omega t} = (e^{i\omega_b t} - e^{i\omega_a t})/it$ and therefore this integral decays as $1/t$. We express $g_{mm'}^{(\alpha)}(\omega)$ as

$$g_{mm'}^{(\alpha)}(\omega) = [u_>(\omega) + u_<(\omega)] + i[v_>(\omega) + v_<(\omega)], \tag{34}$$

where $u_>$ and $v_>$ are positive and $u_<$ and $v_<$ are negative in $\omega_a < \omega < \omega_b$. We write the maximum and minimum of these functions as $u_>^{\max} \equiv \max|u_>(\omega)|$, $u_>^{\min} \equiv \min|u_>(\omega)|$, etc. Then we see the integrals, $\int_{\omega_a}^{\omega_b} d\omega\, u_>^{\min} e^{i\omega t}$, $\int_{\omega_a}^{\omega_b} d\omega\, u_>^{\max} e^{i\omega t}$, etc. also decay as $1/t$. We have

$$\left|\int_{\omega_a}^{\omega_b} d\omega_{mm'}\, u_>^{\min} e^{i\omega_{mm'}t}\right| \le \left|\int_{\omega_a}^{\omega_b} d\omega_{mm'}\, u_>(\omega) e^{i\omega_{mm'}t}\right| \le \left|\int_{\omega_a}^{\omega_b} d\omega_{mm'}\, u_>^{\max} e^{i\omega_{mm'}t}\right|, \tag{35}$$

$$\left|\int_{\omega_a}^{\omega_b} d\omega_{mm'}\, u_<^{\min} e^{i\omega_{mm'}t}\right| \le \left|\int_{\omega_a}^{\omega_b} d\omega_{mm'}\, u_<(\omega) e^{i\omega_{mm'}t}\right| \le \left|\int_{\omega_a}^{\omega_b} d\omega_{mm'}\, u_<^{\max} e^{i\omega_{mm'}t}\right|, \tag{36}$$

etc. Therefore

$$\left|\int_{\omega_a}^{\omega_b} d\omega_{mm'}\, g_{mm'}^{(\alpha)}(\omega) e^{i\omega_{mm'}t}\right| \sim \frac{1}{t}. \tag{37}$$

Thus we have shown

$$|\Delta\sigma_\alpha(t)| \sim \frac{1}{t} \quad (\alpha = x, y). \tag{38}$$

In Figs. 6, 7, and 8, we show logarithmic plots of $|\Delta\sigma_x(t)|$ and $|\Delta\sigma_y(t)|$ in the three cases (i) $p/q = 5/4$ and $m_0 = 2$ ($N_{\mathrm{Ch}} = 2$), (ii) $p/q = 7/6$ and $m_0 = 3$ ($N_{\mathrm{Ch}} = 3$), and (iii) $p/q = 7/6$ and $m_0 = 1$ ($N_{\mathrm{Ch}} = 1$). In all cases, $|\Delta\sigma_x(t)|$ and $|\Delta\sigma_y(t)|$ indeed decay as $1/t$. Thus, the response of the system to the temporal change of the external field disappears in nano-second order even if there is no dissipative mechanism.

Since the correction terms $\Delta\sigma_x(t)$ and $\Delta\sigma_y(t)$ decay as $1/t$, in the limit $t \to \infty$, we obtain

$$j_x(t \to \infty) = \frac{E_y e^2}{2\pi\hbar} N_{\mathrm{Ch}},$$
$$j_y(t \to \infty) = 0. \tag{39}$$

This Hall current was first obtained by Thouless *et al.*[2)]

When the bands $\epsilon_m(\boldsymbol{k})$ and $\epsilon_{m'}(\boldsymbol{k})$ are nearly flat as in the case (iii), we can explicitly calculate the time dependence of $\Delta\sigma_\alpha(t)$. In this case, $\omega_b - \omega_a$ is very small and eq. (33) can be approximated as

$$\Delta\sigma_\alpha(t) \simeq \sum_{m\le m_0}\sum_{m'>m_0} \mathrm{Im}\int_0^{2\pi/b} dk_y\, \tilde{g}_{mm'}^{(\alpha)}(k_y) \int_{\omega_a}^{\omega_b} d\omega_{mm'}\, e^{i\omega_{mm'}t}, \tag{40}$$

where $\tilde{g}_{mm'}^{(\alpha)}(k_y)$ $[= g_{mm'}^{(\alpha)}(\omega_{mm'}, k_y)]$ is independent of $\omega_{mm'}$. We note that

$$\int_{\omega_a}^{\omega_b} d\omega\, e^{i\omega t} = \frac{2}{t}\sin\left(\frac{\omega_b - \omega_a}{2}t\right) e^{i(\omega_b+\omega_a)t/2}. \tag{41}$$

This integral decays as $1/t$ and its amplitude has two kinds of oscillations. The period of one oscillation is inversely proportional to $\omega_b - \omega_a$ and the period of the other is inversely proportional to $\omega_b + \omega_a$. We note that the difference $\omega_b - \omega_a$ is very small and $\omega_a \simeq \omega_b$. Therefore, the frequency of $\exp[i(\omega_b + \omega_a)t/2]$ is given by the energy difference between $\epsilon_m(\boldsymbol{k})$ and $\epsilon_{m'}(\boldsymbol{k})$, and the period of the

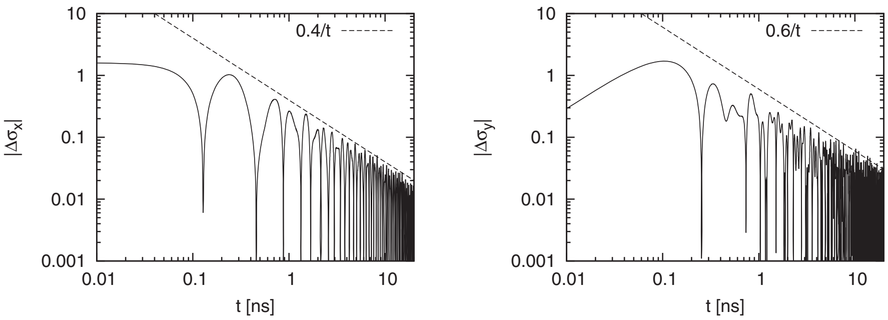

Fig. 6. Case (i): Logarithmic plots of the long-time behavior of $|\Delta\sigma_x(t)|$ and $|\Delta\sigma_y(t)|$. We also draw the dashed lines $0.4/t$ (left) and $0.6/t$ (right) to see $|\Delta\sigma_x(t)|$ and $|\Delta\sigma_y(t)|$ decay as $1/t$. The parameters are the same as in Fig. 2.

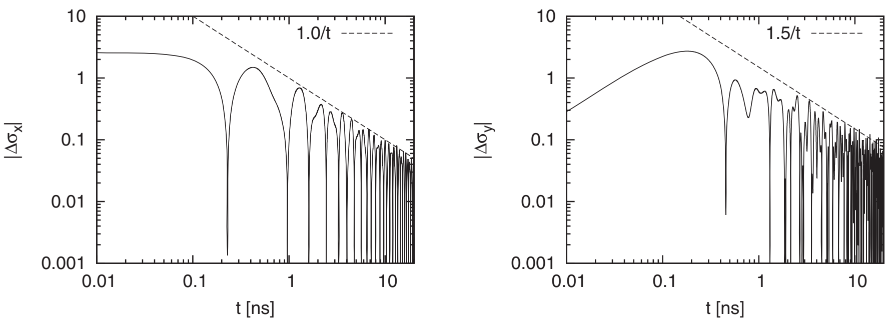

Fig. 7. Case (ii): Logarithmic plots of the long-time behavior of $|\Delta\sigma_x(t)|$ and $|\Delta\sigma_y(t)|$. We also draw the dashed lines $1.0/t$ (left) and $1.5/t$ (right) to see $|\Delta\sigma_x(t)|$ and $|\Delta\sigma_y(t)|$ decay as $1/t$. The parameters are the same as in Fig. 4.

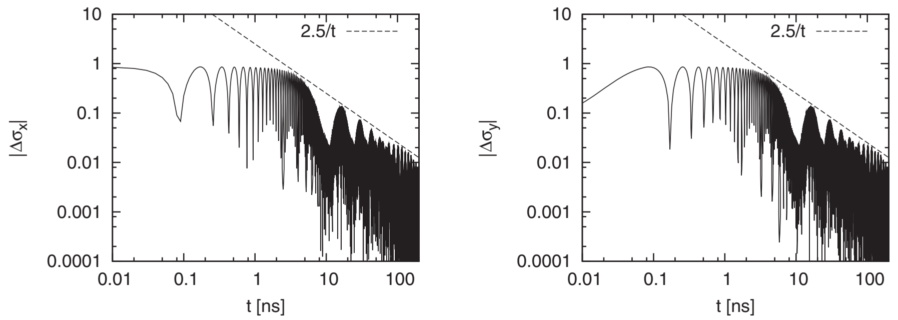

Fig. 8. Case (ii): Logarithmic plots of the long-time behavior of $|\Delta\sigma_x(t)|$ and $|\Delta\sigma_y(t)|$. We also draw the dashed lines $2.5/t$ (left) and $2.5/t$ (right) to see $|\Delta\sigma_x(t)|$ and $|\Delta\sigma_y(t)|$ decay as $1/t$. The parameters are the same as in Fig. 5.

beat $4\pi/(\omega_b - \omega_a)$ is very long. The $1/t$ decay is revealed for a time longer than the period of the beat.

Thus, in nearly flat-band cases, it is easier to observe the $1/t$ dependence because $|\Delta\sigma_x(t)|$ and $|\Delta\sigma_y(t)|$ decay rather slowly and survive for a long time as is seen in Fig. 8.

4. Conclusions

Using the Greenwood linear response theory, we studied the time dependence of the currents in the quantum Hall effect when the electric field is suddenly turned on. We found that both $j_x(t)$ and $j_y(t)$ oscillate because of the quantum fluctuation between two subbands which straddle the Fermi energy. These oscillations decay as $1/t$ and eventually cease. In the limit $t \to \infty$, $j_x(t \to \infty)$ is given as the Chern number N_{Ch} multiplied by e^2/h as Thouless *et al.*[2] obtained. As is discussed in Appendix, the electric fields oscillate in time in the same way as $j_x(t)$ and $j_y(t)$ when, in reverse, the current is applied abruptly at $t = 0$.

We showed that the ratio of the Hall current and the suddenly applied dc field is decomposed into the sum of a constant term and a time-dependent term [eq. (25)]. The constant term is the conductivity for the dc field applied for infinite time and given by the Chern number N_{Ch}. Thus, the time-dependent term $\Delta\sigma_x(t)$ expresses a correction to the Chern number term. In other words, $\Delta\sigma_x(t)$ can be regarded as the fluctuation around the Chern number. It will be remarkable to observe the fluctuation experimentally, since the quantization to the Chern number is normally regarded as very rigid. This fluctuation, which stems from transitions between different subbands, decays as $1/t$.

Thus, the response of the system to the temporal change of the external field decays as $1/t$ even if there is no dissipative mechanism. The amplitude of the decay gets large if the bands that give large contribution to $\Delta\sigma_x(t)$ are nearly flat. In this case, the $1/t$-behavior survives for a long time. In a quantum Hall system on a semiconductor heterojunction, this power-law decay of the order of nano-second might be difficult to observe experimentally because relaxation time due to impurity scattering, etc. is of pico-second order.[31] Cold atomic systems under an artificial magnetic field may overcome these difficulties. In experiments of a Rubidium cold atomic gas trapped by a rotating optical lattice, the time scale of the power-law decay is of the order of millisecond for $a = b \sim 1\,\mu\mathrm{m}$, $U_0 \sim 0.1\,\mathrm{neV}$, and large Ω so that $p/q \sim 1$.

Acknowledgment

One of the authors (M.M.) thanks Dr. Mikito Koshino for indispensable discussions on the numerical calculation of the Hall current. M.M. is also grateful to Professor Piet W. Brouwer for discussion on linear response theory and to Dr. Tomio Y. Petrosky for letting him know the Riemann–Lebesgue theorem. This study is supported by Grants-in-Aid for Scientific Research (Nos. 17340115 and 19740241) from the Ministry of Education, Culture, Sports, Science and Technology as well as by Core Research for Evolutional Science and Technology (CREST) of Japan Science and Technology Agency. The computation in this work was carried out partly on the facilities of the Supercomputer Center, Institute for Solid State Physics, the University of Tokyo.

Appendix: Measuring Electric Fields under an Applied Current

Here, we calculate the voltage for the applied dc current that is switched on abruptly. This situation matches current-controlled experiments. (For theoretical reasons, in the main body of the paper, we calculate the current under the applied voltage.) We find that the voltage also oscillates. Both temporal oscillations of the current and voltage are caused by the quantum fluctuation between two subbands.

We apply the current suddenly at $t = 0$ in the y direction, $j_x(t) = 0$, $j_y(t) = J_y\theta(t)$, and obtain $E_x(t)$ and $E_y(t)$. This may be closer to the experimental situation.

Since we assume linear response, we have ($\alpha = x, y$)

$$j_\alpha(t) = \sum_{\beta=x,y} \int_{-\infty}^{\infty} \mathrm{d}t'\, \sigma_{\alpha\beta}(t - t')E_\beta(t'). \tag{A·1}$$

By the Fourier transform, we obtain

$$\tilde{j}_\alpha(\omega) = \sum_{\beta=x,y} \tilde{\sigma}_{\alpha\beta}(\omega + \mathrm{i}\eta)\tilde{E}_\beta(\omega), \tag{A·2}$$

where $\tilde{j}_\alpha(\omega) = \int j_\alpha(t)\mathrm{e}^{\mathrm{i}\omega t}\,\mathrm{d}t$, etc. We put an infinitesimally small $\eta > 0$ to ensure the causality: $\sigma_{\alpha\beta}(t) = 0$ for $t < 0$. We define the resistivity $\tilde{\rho}_{\alpha\beta}$ as

$$\tilde{E}_\alpha(\omega) = \sum_{\beta=x,y} \tilde{\rho}_{\alpha\beta}(\omega + \mathrm{i}\eta)\tilde{j}_\beta(\omega), \tag{A·3}$$

where

$$\begin{aligned}\tilde{\rho}_{xy}(\omega + \mathrm{i}\eta) &= \frac{-\tilde{\sigma}_{xy}(\omega + \mathrm{i}\eta)}{\tilde{\sigma}_{xy}^2(\omega + \mathrm{i}\eta) + \tilde{\sigma}_{yy}^2(\omega + \mathrm{i}\eta)},\\ \tilde{\rho}_{yy}(\omega + \mathrm{i}\eta) &= \frac{\tilde{\sigma}_{yy}(\omega + \mathrm{i}\eta)}{\tilde{\sigma}_{xy}^2(\omega + \mathrm{i}\eta) + \tilde{\sigma}_{yy}^2(\omega + \mathrm{i}\eta)}.\end{aligned} \tag{A·4}$$

Therefore we obtain electric fields as

$$E_x(t) = \frac{1}{2\pi}\int \mathrm{d}\omega \frac{-\tilde{\sigma}_{xy}(\omega+\mathrm{i}\eta)}{\tilde{\sigma}_{xy}^2(\omega+\mathrm{i}\eta)+\tilde{\sigma}_{yy}^2(\omega+\mathrm{i}\eta)}\tilde{J}_y(\omega)\mathrm{e}^{-\mathrm{i}\omega t}, \quad (\mathrm{A\cdot5})$$

$$E_y(t) = \frac{1}{2\pi}\int \mathrm{d}\omega \frac{\tilde{\sigma}_{yy}(\omega+\mathrm{i}\eta)}{\tilde{\sigma}_{xy}^2(\omega+\mathrm{i}\eta)+\tilde{\sigma}_{yy}^2(\omega+\mathrm{i}\eta)}\tilde{J}_y(\omega)\mathrm{e}^{-\mathrm{i}\omega t}, \quad (\mathrm{A\cdot6})$$

where

$$\tilde{J}_y(\omega) = \frac{\mathrm{i}J_y}{\omega+\mathrm{i}\eta}. \quad (\mathrm{A\cdot7})$$

We obtain the conductivities $\tilde{\sigma}_{xy}(\omega)$ and $\tilde{\sigma}_{yy}(\omega)$ with the help of the calculation in §2. We first note that

$$\tilde{E}_y(\omega) = \int \mathrm{d}t\, E_y\theta(t)\mathrm{e}^{\mathrm{i}(\omega+\mathrm{i}\eta)t} = \frac{\mathrm{i}E_y}{\omega+\mathrm{i}\eta}. \quad (\mathrm{A\cdot8})$$

Using eqs. (25) and (26), we have

$$\begin{aligned}\tilde{\sigma}_{xy}(\omega+\mathrm{i}\eta) &= \frac{\tilde{J}_x(\omega)}{\tilde{E}_y(\omega)} \\ &= \frac{e^2}{2\pi\mathrm{i}\hbar}(\omega+\mathrm{i}\eta)\Bigg[\frac{\mathrm{i}N_{\mathrm{Ch}}}{\omega+\mathrm{i}\eta} + \Bigg(\sum_{m\le m_0}\sum_{m'>m_0} - \sum_{m>m_0}\sum_{m'\le m_0}\Bigg)\int_{\mathrm{MBZ}}\frac{\mathrm{d}^2\boldsymbol{k}}{2\pi}\left\langle\frac{\partial u_{0m}(\boldsymbol{k})}{\partial k_y}\,\middle|\,u_{0m'}(\boldsymbol{k})\right\rangle\left\langle u_{0m'}(\boldsymbol{k})\,\middle|\,\frac{\partial u_{0m}(\boldsymbol{k})}{\partial k_x}\right\rangle \\ &\quad\times\frac{1}{\omega+\mathrm{i}\eta+[\epsilon_{m'}(\boldsymbol{k})-\epsilon_m(\boldsymbol{k})]/\hbar}\Bigg]\end{aligned} \quad (\mathrm{A\cdot9})$$

$$\begin{aligned}\tilde{\sigma}_{yy}(\omega+\mathrm{i}\eta) &= \frac{\tilde{J}_y(\omega)}{\tilde{E}_y(\omega)} \\ &= \frac{e^2}{2\pi\mathrm{i}\hbar}(\omega+\mathrm{i}\eta)\Bigg(\sum_{m\le m_0}\sum_{m'>m_0} - \sum_{m>m_0}\sum_{m'\le m_0}\Bigg)\int_{\mathrm{MBZ}}\frac{\mathrm{d}^2\boldsymbol{k}}{2\pi}\left|\left\langle\frac{\partial u_{0m}(\boldsymbol{k})}{\partial k_y}\,\middle|\,u_{0m'}(\boldsymbol{k})\right\rangle\right|^2 \\ &\quad\times\frac{1}{\omega+\mathrm{i}\eta+[\epsilon_{m'}(\boldsymbol{k})-\epsilon_m(\boldsymbol{k})]/\hbar}.\end{aligned} \quad (\mathrm{A\cdot10})$$

By plugging eqs. (A·9) and (A·10) into eqs. (A·5) and (A·6), we obtain the electric fields:

$$E_x(t) = \frac{2\pi\hbar}{e^2}J_y\int\frac{\mathrm{d}^2\boldsymbol{k}}{\pi}\sum_{m\le m_0}\sum_{m'>m_0}\tilde{S}\left(\frac{\epsilon_{m'}(\boldsymbol{k})-\epsilon_m(\boldsymbol{k})}{\hbar}\right)\mathrm{Im}\left\langle\frac{\partial u_{0m}(\boldsymbol{k})}{\partial k_y}\,\middle|\,u_{0m'}(\boldsymbol{k})\right\rangle\left\langle u_{0m'}(\boldsymbol{k})\,\middle|\,\frac{\partial u_{0m}(\boldsymbol{k})}{\partial k_x}\right\rangle\mathrm{e}^{\mathrm{i}[\epsilon_{m'}(\boldsymbol{k})-\epsilon_m(\boldsymbol{k})]t/\hbar}, \quad (\mathrm{A\cdot11})$$

$$E_y(t) = \frac{2\pi\hbar}{e^2}J_y\int\frac{\mathrm{d}^2\boldsymbol{k}}{\pi}\sum_{m\le m_0}\sum_{m'>m_0}\tilde{S}\left(\frac{\epsilon_{m'}(\boldsymbol{k})-\epsilon_m(\boldsymbol{k})}{\hbar}\right)\left|\left\langle\frac{\partial u_{0m}(\boldsymbol{k})}{\partial k_y}\,\middle|\,u_{0m'}(\boldsymbol{k})\right\rangle\right|^2\sin\left\{\frac{[\epsilon_{m'}(\boldsymbol{k})-\epsilon_m(\boldsymbol{k})]t}{\hbar}\right\}, \quad (\mathrm{A\cdot12})$$

where

$$\tilde{S}(\omega)^{-1} = -\left(\frac{2\pi\hbar}{e^2}\right)^2\left[\tilde{\sigma}_{xy}^2(\omega)+\tilde{\sigma}_{yy}^2(\omega)\right]. \quad (\mathrm{A\cdot13})$$

Note that $E_x(t)$ and $E_y(t)$ have the same time dependence as $j_x(t)$ and $j_y(t)$ in §2; the period of the oscillation is dominantly given by the energy difference between two subbands which straddle the Fermi energy.

1) R. E. Prange and S. M. Girvin: *The Quantum Hall Effect* (Splinger-Verlag, New York, 1987).
2) D. J. Thouless, M. Kohmoto, M. P. Nightingale, and M. den Nijs: Phys. Rev. Lett. **49** (1982) 405.
3) J. Avron, R. Seiler, and B. Simon: Phys. Rev. Lett. **51** (1983) 51.
4) Q. Niu, D. J. Thouless, and Y.-S. Wu: Phys. Rev. B **31** (1985) 3372.
5) H. Aoki and T. Ando: Phys. Rev. Lett. **57** (1986) 3093.
6) K. Ishikawa and T. Matsuyama: Z. Phys. C **33** (1986) 41.
7) K. Ishikawa and T. Matsuyama: Nucl. Phys. B **280** (1987) 523.
8) N. Imai, K. Ishikawa, T. Matsuyama, and I. Tanaka: Phys. Rev. B **42** (1990) 10610.
9) M. Kohmoto: Ann. Phys. (N.Y.) **160** (1985) 343.
10) M. Kohmoto: Phys. Rev. B **39** (1989) 11943.
11) Y. Hatsugai: J. Phys.: Condens. Matter **9** (1997) 2507.
12) J. Goryo and M. Kohmoto: cond-mat/0606758.
13) S. Tung, V. Schweikhard, and E. A. Cornell: Phys. Rev. Lett. **97** (2006) 240402.
14) D. Jaksch and P. Zoller: New J. Phys. **5** (2003) 56.
15) E. J. Mueller: Phys. Rev. A **70** (2004) 041603.
16) D. R. Hofstadter: Phys. Rev. B **14** (1976) 2239.
17) C. T. Liu, D. C. Tsui, M. Shayegan, K. Ismail, D. A. Antoniadis, and H. I. Smith: Appl. Phys. Lett. **58** (1991) 2945.
18) M. C. Geisler, J. H. Smet, V. Umansky, K. von Klitzing, B. Naundorf, R. Ketzmerick, and H. Schweizer: Phys. Rev. Lett. **92** (2004) 256801.
19) M. C. Geisler, S. Chowdhury, J. H. Smet, L. Höppel, V. Umansky, R. R. Gerhardts, and K. von Klitzing: Phys. Rev. B **72** (2005) 045320.
20) M. Machida, N. Hatano, and J. Goryo: J. Phys. Soc. Jpn. **75** (2006) 063704.
21) H. Nakano: Prog. Theor. Phys. **15** (1956) 77.
22) R. Kubo: Can. J. Phys. **34** (1956) 1274.
23) R. Kubo: J. Phys. Soc. Jpn. **12** (1957) 570.
24) D. A. Greenwood: Proc. Phys. Soc. **71** (1958) 585.
25) L. D. Landau and E. M. Lifshitz: *Mechanics* (Butterworth-Heinemann, Oxford, U.K., 1976) 3rd ed.
26) B. P. Anderson and M. A. Kasevich: Science **282** (1998) 1686.
27) K. W. Madison, C. F. Bharucha, P. R. Morrow, S. R. Wilkinson, Q. Niu, B. Sundaram, and M. G. Raizen: Appl. Phys. B **65** (1997) 693.
28) M. Koshino and T. Ando: J. Phys. Soc. Jpn. **73** (2004) 3243.
29) M. Koshino and T. Ando: Phys. Rev. B **73** (2006) 155304.
30) I. S. Gradshteyn and I. M. Ryzhik: *Table of Integrals, Series, and Products* (Academic Press, San Diego, CA, 1994) 5th ed., p. 1133.
31) P. T. Coleridge: Phys. Rev. B **44** (1991) 3793.